Performance Based Assessment And Retrofit Of Nonductile Existing Reinforced Concrete Structures

Andrea Miano[1], Halil Sezen[2], Fatemeh Jalayer[1], and Andrea Prota[1]

[1]Department of Structures for Engineering and Architecture, University of Naples "Federico II", Via Claudio 21, 80125, Naples, Italy; {andrea.miano, fatemeh.jalayer, a.prota}@unina.it
[2]Department of Civil, Environmental & Geodetic Engineering, Ohio State University Neil Avenue 2070, 43210, Columbus, Ohio, USA; sezen.1@osu.edu

ABSTRACT

In different high seismic regions around the world, post-earthquake reconnaissance has shown that nonductile concrete frame structures are much more susceptible to collapse than modern code-conforming frames. Therefore, for this type of structures, it is necessary to accurately model materials and members to capture the flexure, shear, and flexure-shear failure modes in members and the potential collapse of the structure. In this paper, alternative retrofit methods are evaluated for these older frame buildings using a probability-based framework, based on nonlinear dynamic Cloud Analysis, in order to assess the structural performance and safety at each chosen performance level. As a case study, the longitudinal frame of an existing building is modeled, including the effect of flexural-shear-axial load interaction and the longitudinal bar slip deformation component in order to be able to capture column shear and axial failures. The critical demand to capacity ratio, corresponding to the component or mechanism that leads the structure closest to the onset of limit state (e.g., near collapse), is adopted as the structural response parameter. This structural response parameter, that is equal to unity at the onset of limit state, can encompass both ductile and brittle failure mechanisms. It can also register a possible shift in the governing failure mechanism with increasing intensity. Finally, the estimates of expected life cycle cost are compared for the retrofit methods considered in this research.

INTRODUCTION

Major earthquakes that hit different countries around the world in the past years have shown the vulnerability and deficiencies of existing structures including nonductile reinforced concrete (RC) frame buildings. These nonductile concrete frame structures are much more prone to collapse with respect to the modern code-conforming frames (Sezen et al. 2003, and Liel et al. 2009). Since these buildings comprise large percentage of existing building stock, efficient assessment methods are needed to compare different retrofit methods and to predict the collapse risk of existing structures in seismic regions (Zareian and Krawinkler 2007, and Eads et al. 2013). Different conventional retrofit methods, such as concrete or steel jacketing of the columns, addition of shear walls and new methods often based on new materials, such as fiber reinforced polymers (FRP), have been proposed (Moehle 2000 and Thermou and Elnashai 2005). These methods can be applied considering the desired performance level, requirements of new seismic codes reduction in probability of collapse, optimization of cost and/or minimization of losses.

In this paper, alternative retrofit methods are evaluated for older nonductile frame buildings using a nonlinear structural performance assessment methodology. Nonlinear dynamic analysis procedures can be used to perform probabilistic seismic assessment, using recorded ground motions. These procedures can be used to estimate parameters required for

specific probabilistic assessment criteria, such as Demand and Capacity Factored Design (DCFD, Cornell et al. 2002), and also to make direct probabilistic performance assessment using numerical methods (Shome et al. 1998, Vamvatsikos and Cornell 2002, Cornell et al. 2002, Baker and Cornell 2005, and Jalayer and Cornell 2009). In particular, Cloud Analysis is chosen here by applying simple regression in the logarithmic space of nonlinear dynamic structural response versus seismic intensity for a set of ground motion records. The simplicity of its formulation makes it a quick and efficient analysis procedure for fragility assessment and/or performance based safety-checking (Celik and Ellingwood 2010, Jalayer et al. 2007, 2015 and 2017). Based on this probabilistic nonlinear dynamic analysis framework, a risk based retrofit strategy optimization is developed in this study. A seven-story hotel building in Van Nuys, California, is used as a case study in this research. The RC frame building suffered significant damage during the 1994 Northridge earthquake. A perimeter longitudinal frame of the building is modeled as built and retrofitted, including the effect of flexural-shear-axial load interaction to be able to capture column shear and axial failures.

The goal of this research is to propose a nonlinear performance-based methodology in order to compare different retrofit methods considering hazard level, target performance levels and also life cycle costs. The methodology is illustrated using three retrofit strategies for the analyzed case study frame, used to improve the seismic performance of the frame. In particular, strictly speaking, performance-based retrofit design should lead to the optimal retrofit strategy by comparing the expected loss during the service life of the structure for each viable retrofit option, based on risk-related safety-checking criteria. In summary, the performance-based procedure implemented in this paper identifies the most economic retrofit solution that satisfies structural safety requirements for a given performance level. However, the novelty of the proposed research is not in the evaluation of the specific retrofit solutions for the case study, but in the critical process proposed to evaluate the effectiveness of different retrofit methods using a performance based approach.

1. METHODOLOGY

1.1 The structural performance variable

As described in Jalayer et al. (2007), for each nonlinear time-history analysis, the corresponding critical demand to capacity ratio (DCR_{PL}), equal to the mechanism that brings the structure closest to the onset of the specific performance level *PL*, is adopted as the structural response parameter. The DCR_{PL} parameter, that is equal to unity at the onset of performance level, can account for both ductile and brittle failure mechanisms. It is defined as:

$$DCR_{PL} = \max_{l}^{N_{mech}} \min_{j}^{N_l} \frac{D_{jl}}{C_{jl}(PL)} \tag{1}$$

where N_{mech} is the number of considered potential failure mechanisms; N_l is the number of components taking part in the lth mechanism; D_{jl} is the demand evaluated for the jth structural component of the lth mechanism; $C_{jl}(PL)$ is the performance level capacity for the jth component of the lth mechanism. The capacity values refer to the Immediate Occupancy PL, Life Safety PL and Collapse Prevention PL, as described in Table C2.1 of ASCE 41 (2013) in this work, but the procedure can be used for any other prescribed performance levels or limit states. In DCR_{PL} definition, *D* is the demand expressed in terms of maximum chord rotation for the component, denoted as $\theta_{D,\max}$, and computed from nonlinear dynamic analysis, while for C: a) *Immediate Occupancy Performance Level: C* is the component chord rotation capacity, denoted as $\theta_{C,\text{yielding}}$, and identified as the deformation capacity corresponding to the point in the force-deformation curve of the member in which the longitudinal steel rebar in the member starts to yield in tension; b) *Life Safety Performance Level: C* is the component chord

rotation capacity, $\theta_{C,\text{ultimate}}$, and identified as deformation capacity corresponding to the point in the force-deformation curve of the member, where a 20% degradation or reduction in the maximum strength takes place; c) *Collapse Prevention Performance Level: C* is the component chord rotation capacity, denoted as $\theta_{C,\text{axial}}$, and identified as the deformation capacity corresponding to the point in the force-deformation curve of the member associated with the complete loss of vertical-load carrying capacity (to account for the loss of axial load bearing capacity).

1.2 Cloud Analysis considering collapse and/or global dynamic instability

In order to estimate the structural fragility, *Cloud* analysis is adopted herein for nonlinear dynamic analysis procedures. Cloud analysis is a procedure in which a structure is subjected to a set of ground motion records of different first-mode *Sa(T)* values. Once the ground motion records are selected, they are applied to the structure and the resulting *DCR* is calculated. This provides a set of values that form the basis for the cloud-method calculations. The cloud data can be separated to two parts: (a) *NoC* data which correspond to that portion of records for which the structure does not experience "*Collapse*", (b) *C* data for which the structure leads to "Collapse" (the criteria for defining Collapse cases are presented in Miano et al. 2017a and 2017b). In order to estimate the statistical properties of the cloud response, with respect to *NoC* data, conventional linear regression is applied to the response on the natural logarithmic scale, which is the standard basis for the underlying log-normal distribution model. This is equivalent to fitting a power-law curve to the cloud response in the original (arithmetic) scale. This results in a curve that predicts the median drift demand for a given level of structural acceleration:

$$\begin{aligned} &\eta_{DCR|Sa,NoC}(Sa) = a \cdot Sa^{b} \\ &\ln(\eta_{\text{DCR}|Sa,NoC}(Sa)) = \ln(a) + b \cdot \ln(Sa) \end{aligned} \tag{2}$$

where *ln(a)* and *b* are regression constants. The logarithmic standard deviation $\beta_{\text{DCR}|Sa,NoC}$ is the root mean sum of the square of the residuals with respect to the regression prediction:

$$\beta_{DCR|Sa,NoC} = \sqrt{\frac{\sum(\ln(DCR_i) - \ln(a \cdot S_{a,i}{}^{b}))^2}{N_{NoC} - 2}} \tag{3}$$

where DCR_i and $S_{a,i}$ are the demand over capacity ratio values and the corresponding spectral acceleration for record number *i* within the cloud response set and N_{NoC} is the number of *NoC* records. The standard deviation of regression, as introduced in the preceding equation, is presumed to be constant with respect to spectral acceleration over the range of spectral accelerations in the cloud. The fragility, expressed generally as the conditional distribution of *DCR* given *Sa*, can be expanded with respect to *NoC* and *C* data as follows using Total Probability Theorem (see Jalayer and Cornell 2009, Jalayer et al. 2017):

$$P\left(DCR_{LS} > 1 \middle| S_a\right) = P\left(DCR_{PL} > 1 \middle| S_a, NoC\right) \cdot \left(1 - P(C \middle| S_a)\right) + P\left(DCR_{PL} > 1 \middle| S_a, C\right) \cdot P\left(C \middle| S_a\right) \tag{4}$$

The *NoC* term $P(DCR>1|Sa,NoC)$ is the conditional distribution of *DCR* given *Sa* and *NoC*, and can be described by a lognormal distribution (Jalayer and Ebrahimian 2017):

$$P\left(DCR_{PL} > 1 \middle| S_a, NoC\right) = \Phi\left(\frac{\ln \eta_{DCR_{PL}|S_a,NoC}}{\beta_{DCR_{PL}|S_a,NoC}}\right) \tag{5}$$

where Φ is the standardized Gaussian cumulative distribution function (CDF) and $\eta_{DCR|Sa,NoC}$ and $\beta_{DCR|Sa,NoC}$ are presented in Eqs. (2) and (3). The term $P(C|Sa)=1-P(NoC|Sa)$ is probability of global dynamic instability (Collapse), which can be expressed by a logistic regression model (a.k.a., logit) on the *Sa* values of the entire cloud data:

$$P\left(C \mid Sa\right) = \frac{1}{1 + e^{-\left(\beta_0 + \beta_1 . Sa\right)}} \tag{6}$$

where β_0 and β_1 are the parameters of the logistic regression. It should be noted that the logistic regression model belongs to the family of generalized regression models and is particularly useful for cases in which the regression dependent variable is binary (i.e., can have only two values 1 and 0, *yes* or *no*, which is the case of *C* and *NoC* herein).

1.3 Performance-based safety-checking framework

As described in Jalayer and Cornell (2003), a framework for probability-based demand and capacity factor design (*DCFD*) seismic safety evaluation is implemented in order to verify the structural safety at each performance level. The *DCFD* format is based on a closed-form analytical expression for the mean annual frequency of exceeding a structural performance level. The threshold for each performance level is identified by a critical demand to capacity ratio DCR_{PL} calculated for the prescribed performance level and set equal to unity. According to *DCFD*, the structure in question satisfies the safety requirements for a prescribed performance level *PL* if the seismic demand corresponding to an acceptable risk level is less than or equal to the seismic capacity for that *PL*. Herein, an intensity-based version of this format is adopted where the safety criteria is expressed in term of the seismic intensity measure (see Jalayer et al. 2016):

$$S_a(P_o) \le S_a^{PL} \tag{7}$$

where $S_a(P_o)$ or the intensity measure (IM)-based *factored demand* (denoted generically later as D_{PL}, where *PL=IO, LS, CP*) is the spectral acceleration value corresponding to the acceptable probability level P_o, based on the site-specific mean hazard curve (which can be obtained from https://www.usgs.gov) for the fundamental period of the frame. The hazard curve is approximated by a power-law type of expression in the region of spectral acceleration values of interest:

$$S_a(P_o) = \lambda^{-1}_{S_a}(P_o) \;;\; \lambda_{S_a}(S_a) \approx k_o \cdot S_a^{-k} \tag{8}$$

where k_o and k are the fit parameters with k that is the slope of this approximate curve. S_a^{PL} (denoted generically later as C_{PL}) is the IM-based *factored capacity* and is calculated as:

$$S_a^{PL} = \eta(S_a^{DCR_{PL}=1}) \cdot \exp\left(-\frac{k}{2}\beta(S_a^{DCR_{PL}=1})^2\right) \tag{9}$$

where $S_a^{DCRPL=1}$ is the spectral acceleration at the onset of performance level *PL* (DCR_{PL}=1); $\eta(S_a^{DCRPL=1})$ and $\beta(S_a^{DCRPL=1})$ are the median and logarithmic standard deviation of the fragility curve for performance level *PL*. The fragility, defined as $P(DCR_{PL} > 1 | S_a)$ is a lognormal cumulative distribution function with median and logarithmic standard deviation equal to:

$$\eta(S_a^{DCR_{PL}=1}) = S_a^{50th} \;;\; \beta(S_a^{DCR_{PL}=1}) = \frac{1}{2}\ln\frac{S_a^{84th}}{S_a^{16th}} \tag{10}$$

where S_a^{16th}, S_a^{50th}, S_a^{84th} are the values of S_a corresponding to probability values equal to 0.16, 0.50 and 0.84, respectively.

2. CASE STUDY AND MODEL DESCRIPTION

2.1 Building description

One of the longitudinal frames of the seven-story Holiday Inn hotel building in Van Nuys, California, is modeled in this study (Figure 1). Columns in the longitudinal frame are 356 mm wide and 508 mm deep, i.e., they are oriented to bend about their weak axis when resisting lateral forces. Spandrel beams in the north frame are 406 mm wide and 762 mm deep in the second floor, 406 mm by 572 mm in the third through seventh floors, and 406 mm by 559 mm at the roof level. Column concrete has a nominal compressive strength f'_c of 34.5 MPa in the first story, 27.6 MPa in the second story, and 20.7 MPa in other floors. Beam and slab concrete

strength f'_c is 27.6 MPa in the second floor and 20.7 MPa in other floors. Grade 60 (f_y=414 MPa) reinforcing steel is used in columns. The specified yield strength, f_y, is 276 MPa (Grade 40) for the steel used in beams and slabs.

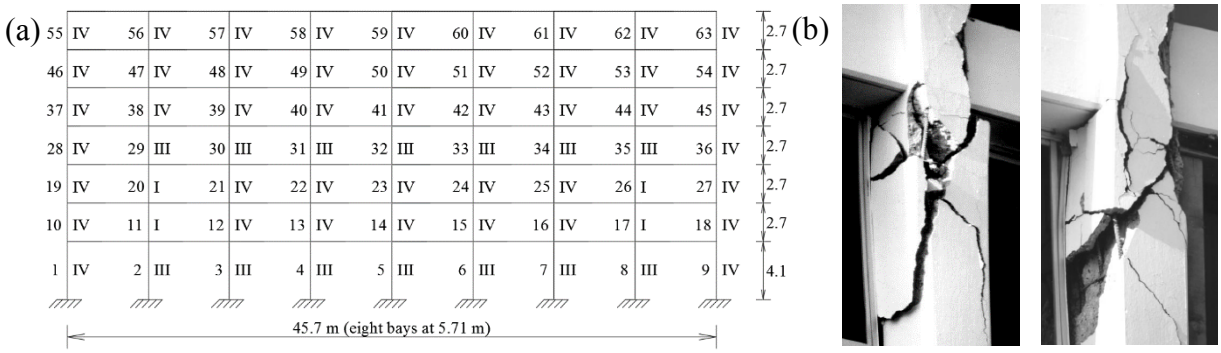

Figure 1. (a) Holiday Inn hotel longitudinal building frame and (b) some of the damaged columns in this frame after the 1994 Northridge earthquake (Trifunac et al. 1999)

In the frame modeled in this study (Figure 1a), end columns include eight 28.7 mm diameter longitudinal (No.9) bars between ground and second floors and six 22.2 mm diameter (No.7) bars in other stories. The 9.5 mm diameter (No.3) column ties are spaced at 310 mm on center between ground and second floors and 6.4 mm diameter (No.2) ties are spaced at 310 mm on center above the second floor level. All middle columns are reinforced with ten No.9 longitudinal bars between ground and second floor, six No.9 bars between second and fourth floors and six No.7 bars above the fourth floor (with the exception of columns 11, 17, 20 and 26, which are reinforced with eight No.9 bars between second and fourth floors). The No.3 and No.2 column ties are spaced at 310 mm below and above the fourth floor level, respectively. Beams are reinforced with two 19.1 mm diameter (No.6) longitudinal bars at the bottom, and top reinforcement varies between two No.8 and three No.9. The stirrups are No.3 spaced at 310 mm on center above the ground level. Other column and beam reinforcement details are provided in Krawinkler (2005).

2.2 Modeling of materials and building frame

The Holiday Inn hotel building experienced multiple shear failures in the columns of the north longitudinal frame, during the 1994 Northridge earthquake (Krawinkler 2005). It is necessary to model materials and column members to capture the shear and the flexure-shear failure modes in columns and the potential collapse of the longitudinal frame (see Miano et al. 2017a and 2017b for more details). About flexural model, unidirectional axial behavior of concrete and steel are modeled to simulate the nonlinear response of beams and columns. Concrete material response is simulated using the Concrete01 material model in OpenSees (McKenna 2011), which includes zero tensile strength and a parabolic compressive stress-strain behaviour up to the point of maximum strength with a linear deterioration beyond peak strength. Longitudinal reinforcing steel behavior is simulated using the Steel02 material in OpenSees, which includes a bilinear stress-strain envelope with a curvilinear unload-reload response under cyclic loading.

Flexural response of beams and columns response is simulated using uniaxial fibers within the gross cross section were assigned either concrete or steel. A typical column cross section included 30 layers of axial fibers, parallel to the depth of the section. Figure 2a shows the moment-curvature relationship for a selected column (second column on the left in the second story and third column on the left in the third story in Figure 1a), obtained from a fiber cross section analysis. In force-based column elements, distributed plasticity model is used in OpenSees in order to allow for yielding and plastic deformations at any integration point along

the element length under increasing loads. Newton-Cotes integration (Scott and Fenves 2006) is selected. This method distributes integration points uniformly along the length of the element, including one point at each end of the element (Figure 2b). Beams member force-deformation response is computed assuming that inelastic action occurs mainly at the member ends and that the middle of the member remains typically elastic. Modified Gauss Radau integration (Scott and Fenves 2006) is selected. This method presents two integration points at the element ends and at 8/3 of the hinge length, $L_0=h$, from the end of the element (Figure 2c).

The shear model by (Setzler and Sezen 2008) can capture the shear response with a lateral force-shear displacement envelope, that includes three distinct points corresponding to: 1) Maximum shear strength and corresponding shear displacement; 2) Onset of shear strength degradation and corresponding displacement; 3) Shear displacement at axial load failure. The shear strength is calculated according to the model by Sezen and Moehle (2004). The shear displacement at peak strength is calculated as in (Sezen 2008). As described in (Setzler and Sezen 2008), the shear displacement at the onset of shear failure is adopted from (Gerin and Adebar 2004). Shear displacement at axial failure is obtained using the procedure given in (Setzler and Sezen 2008), using total lateral displacement, obtained with the equation proposed by Elwood and Moehle 2005. About bar slip model, slip of column reinforcing bars at column ends causes rigid body rotation of the column. This rotation is not accounted for in flexural analysis, where the column ends are assumed to be fixed. The bar slip model used in this study was originally developed by (Sezen and Moehle 2003) and presented in (Setzler and Sezen 2008). This model assumes a stepped function for bond stress between the concrete and reinforcing steel over the embedment length of the bar. The rotation due to slip, θ_s, is calculated as *slip/(d-c)*, where slip is the extension of the outermost tension bar from the column end and d and c are the distances from the extreme compression fiber to the centroid of the tension steel and the neutral axis. The column lateral displacement due to bar slip is equal to the product of the slip rotation and the column length.

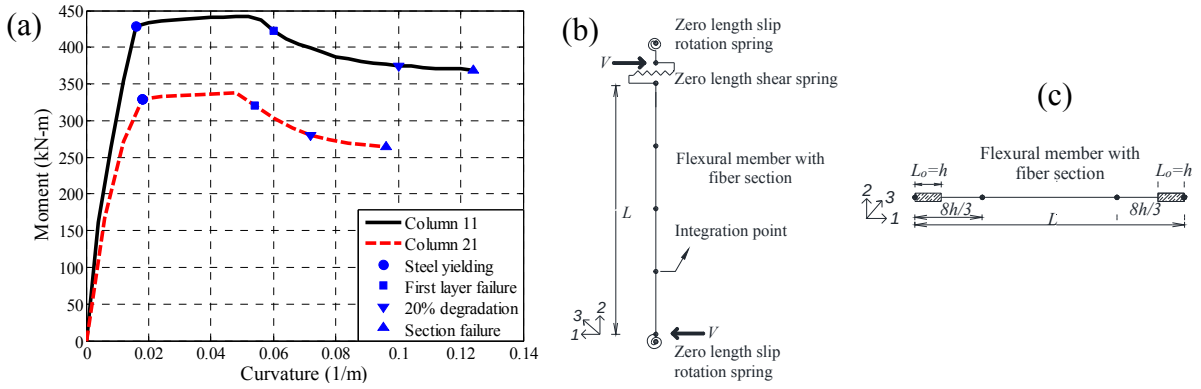

Figure 2. (a) Moment-curvature relationship for a single column (second column on the left in the second story and third column on the left in the third story in Figure 1a); spring model used for (b) column with fixed ends, and (c) beam with fixed ends.

The total lateral response of a RC column can be modeled using a set of springs in series in OpenSees. The flexure, shear and bar slip deformation models discussed above are each modeled by a spring or element (Figure 2b). Each spring is subjected to the same lateral force. Initially, the total displacement response is the sum of the responses of each spring. The combined column spring model is shown in Figure 2b. A typical column element includes two zero-length bar slip springs at its ends, one zero-length shear spring and a flexural element with five integration points. The shear behavior is modeled as a uniaxial hysteretic material defined for the spring in the shear direction (i.e., transverse direction of the column or direction 1 in Figure 2c). The bar slip rotation is modeled with two rotational springs at the column ends

using a uniaxial hysteretic material (i.e., direction 3 in Figure 2c). Finally, same vertical displacement is maintained between nodes of zero length elements in the vertical direction (i.e., direction 2 in Figure 2c), using the equalDOF option in OpenSees. The three deformation components are added together to predict the total response up to the peak strength of the column. Rules are established for the post-peak behavior of the springs based on a comparison of the shear strength V_n, the yield strength V_y (the shear strength corresponding to moment capacity M_y at first longitudinal steel yielding, $V_y=2M_y/L$), and the flexural strength V_p ($V_p=2M_p/L$ for a fixed ended column with maximum flexural strength of M_p) required to reach the plastic moment capacity. By comparing V_n, V_y, and V_p, the columns are classified into different categories (Setzler and Sezen 2008). Figure 3a shows the deformation components and the total lateral displacement for a column of the frame, belonging to Category I (shear critical members).

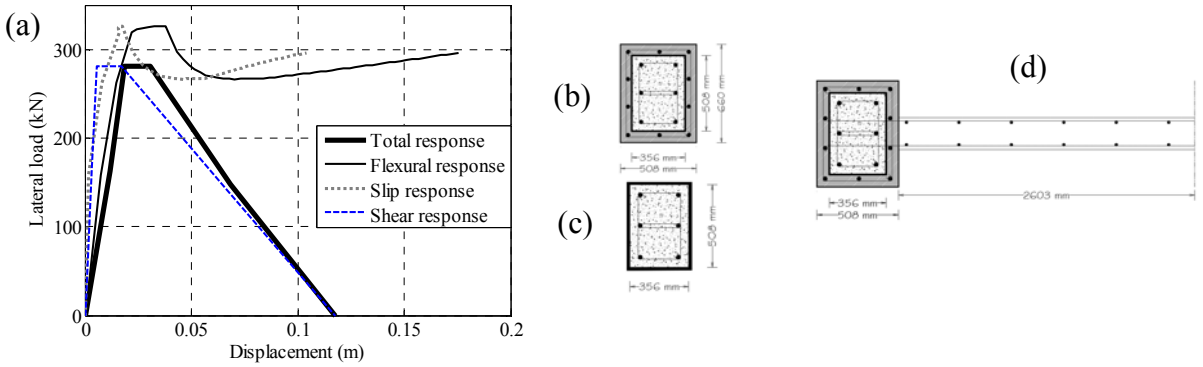

Figure 3. (a) Three different deformation components and the total lateral displacement for columns 11 of the frame (Figure 1a), belonging to Category I (shear critical); (b) RC jacketing of columns, (c) FRP wrapping of columns, and (d) shear wall addition.

2.3 Models for retrofitted frames

The main goal of the retrofit design is to prevent premature failure of brittle elements and to increase their ductility and strength. In addition, the lateral displacements need to be as uniform as possible over the height of the structure to avoid concentration of inelastic deformations in a single story to prevent soft story mechanism. In general, there are many practical retrofit options (Moehle 2000 and Thermou and Elnashai 2005). However, in this work three common strategies are considered to show the effectiveness of different retrofit options, while stressing the critical process of performance based assessment: 1) RC jacketing of the columns, 2) addition of new shear walls into the frame, and 3) FRP wrapping of the columns. A target drift capacity is herein adopted as retrofit design criterion. This criterion is very helpful in terms of feeding an intelligent first guess into the procedure. Such a first guess is assessed based on performance-based criteria (Cornell and Krawinkler 2000, ASCE 41 2013 and Fardis 2009). The performance-based procedure implemented in this paper identifies, however, the most economic retrofit solution that satisfies structural requirements for a given performance level.

The first retrofit scheme considered is the reinforced concrete jacketing of all columns in the frame. Two different schemes of RC jacketing of the columns are selected, based on the consideration that the retrofit of a building should be seen as an iterative process: a) all columns of the frame are RC jacketed; and b) all columns of the first five floors of the frame are RC jacketed. Figure 3b shows the retrofitted cross section for a central column in the fourth story (Miano et al. 2017a and 2017b for more details). The second retrofit method is the addition of a new shear wall into the frame The wall is centered on the frame and is doweled into the existing columns and beams. Figure 3c shows the shear wall cross section in the fourth floor (see Miano et al.2017a and 2017b). In the third retrofit application, the columns of the frame

are wrapped with carbon fiber reinforced polymer composite (CFRP) as shown in Figure 3d for a central column in the fourth story (Miano et al.2017a and 2017b). The columns are wrapped following two schemes: a) all columns are wrapped with only one layer of uni-axial transverse CFRP; and b) all columns are FRP wrapped, but for the central columns in the first floor two FRP layers are used.

3. CASE STUDY RESULTS

3.1 Cloud Analysis

A set of 70 strong ground-motion records are selected from the NGA-West2 database in order to implement Cloud Analysis. This suite of records is presented in detail in Jalayer et al. 2017. The Cloud response is obtained by applying original ground motions to the structure. Once the ground motion records are applied to the structure, the resulting $DCR_{PL}=D/C$ are calculated for each performance level. Figures 4, 5, 6 and 7 show the Cloud Analysis results for the different performance levels for the bare frame and for one scheme of each retrofit option. The gray-colored circles represent the *NoC* data, while the gray colored with red edge squares represent the *C* data (Section 1.2). Figures also show the 16th, 50th and 84th percentiles of the performance variable as function of *Sa* and report the parameters of the logarithmic linear regression (considering only the *NoC*), namely, *log a*, *b* and standard deviation $\beta_{DCRPL|Sa,\ NoC}=\beta$.

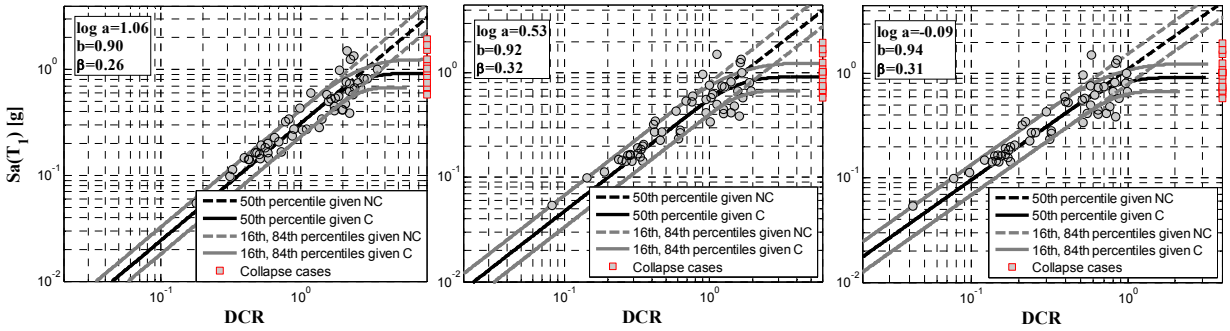

Figure 4. Cloud regression for bare frame: (a) immediate occupancy *PL*, (b) life safety *PL*, and (c) collapse prevention *PL*.

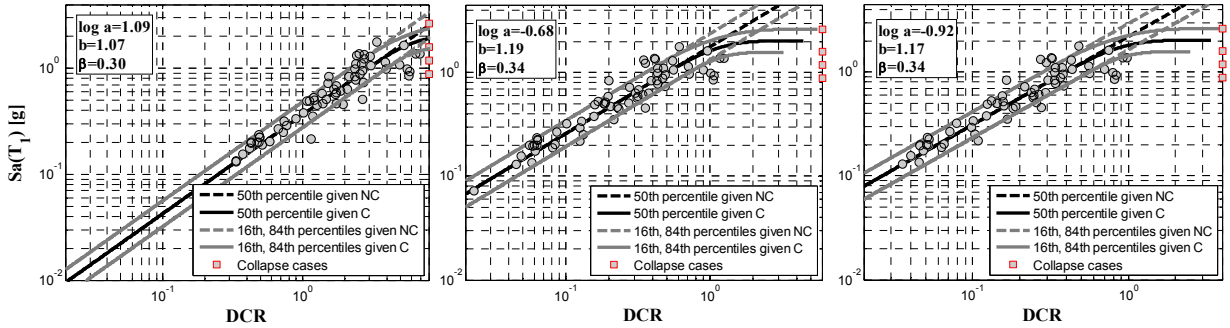

Figure 5. Cloud regression for RC jacketing (scheme a): (a) immediate occupancy *PL*, (b) life safety *PL*, and (c) collapse prevention *PL*.

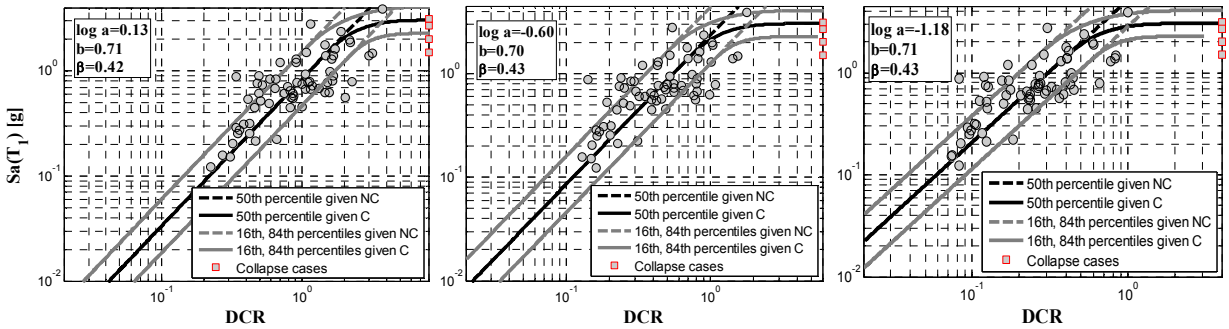

Figure 2. Cloud regression for shear wall: (a) immediate occupancy *PL*, (b) life safety *PL*, and (c) collapse prevention *PL*.

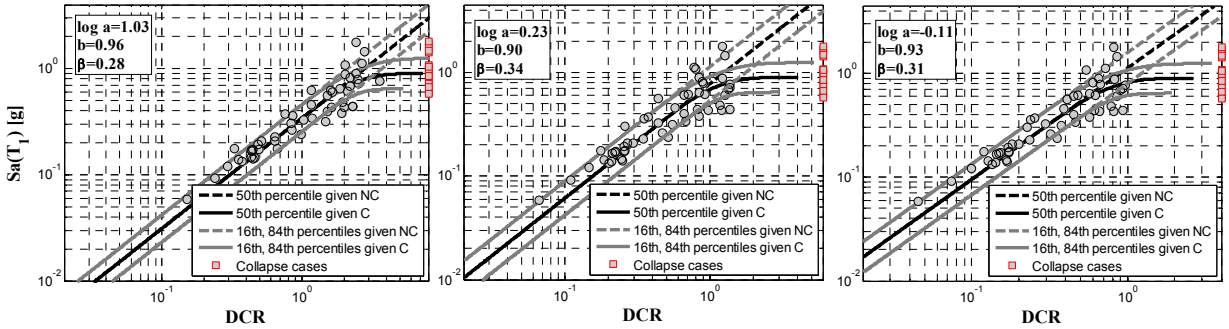

Figure 7. Cloud regression for FRP wrapping (scheme a): (a) immediate occupancy *PL*, (b) life safety *PL*, and (c) collapse prevention *PL*.

3.2 Performance-based safety-checking

The framework for probability-based demand and capacity factor design (*DCFD*) seismic safety evaluation (Section 1.3) is adopted here to verify the structural safety at each performance level. Figure 8 shows the mean hazard curves (https://www.usgs.gov), the fragility curves and the calculation of D_{PL} $S_a(P_o)$ and $C_{PL}=S_a^{PL}$ for all the performance levels.

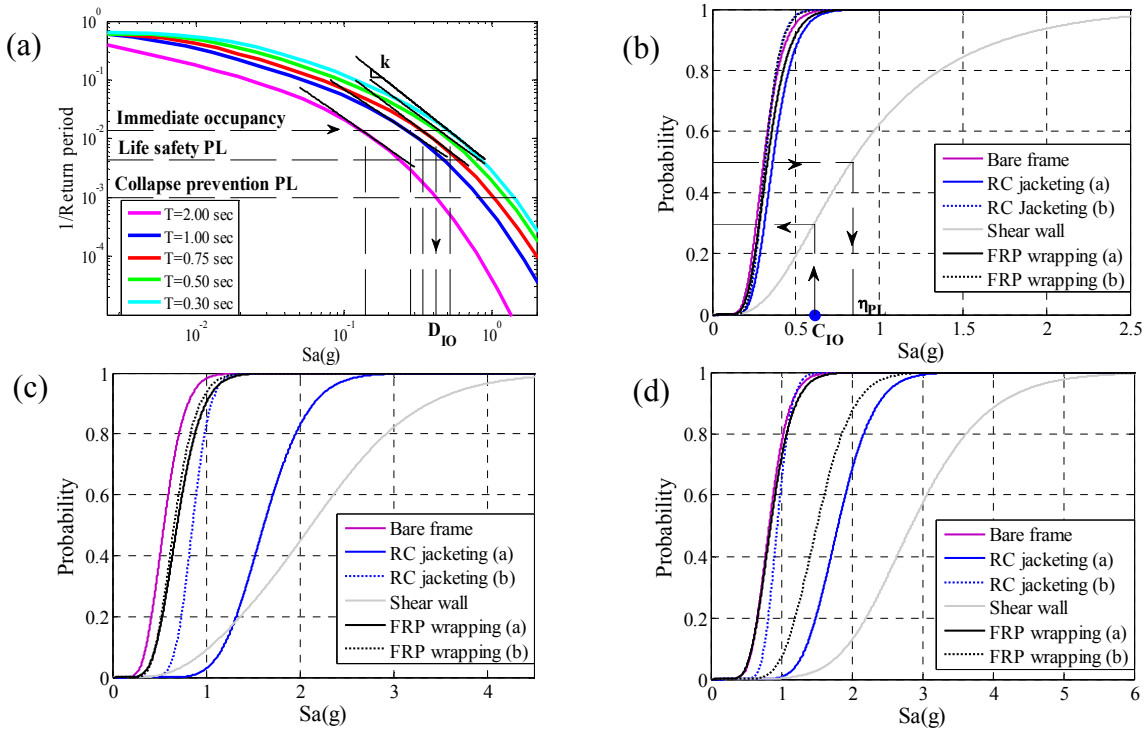

Figure 8. (a) Mean hazard curve and calculation of D_{PL}; fragility curves and calculation of C_{PL} for (b) immediate occupancy, (c) life safety and (d) collapse prevention *PLs*.

Table 1 shows the comparison between D_{PL} and C_{PL}, respectively, for each modeling option in each performance level. For the immediate occupancy *PL*, the frame with shear wall achieves the biggest factored capacity, that is about four times that of the bare frame. For the life safety and the collapse prevention *PLs,* different schemes belonging to the different retrofit options are able to lead to a factored capacity sensibly higher than the corresponding factored demand. It is to note that the retrofit schemes not able to satisfy the safety condition for all the performance levels are not included in the comparison in terms of life cycle cost.

Table 1. Comparison between D_{PL} and C_{PL} for each modelling option in each performance level

Model	$Sa\ (T_1)$ (g)	D_{IO} (g)	C_{IO} (g)	D_{LS} (g)	C_{LS} (g)	D_{CP} (g)	C_{CP} (g)
Bare frame	1.17	0.27	0.27	0.45	0.48	0.78	0.73
RC jacketing (a)	0.93	0.30	0.34	0.51	1.51	0.89	1.68
RC jacketing (b)	0.95	0.29	0.31	0.50	0.78	0.87	0.87
Shear wall	0.54	0.44	0.61	0.75	1.65	1.28	2.48
FRP wrapping (a)	1.13	0.27	0.32	0.45	0.62	0.78	0.76
FRP wrapping (b)	1.13	0.27	0.30	0.45	0.61	0.78	1.33

4. LIFE CYCLE COST ANALYSIS

The expected life cycle cost is an important parameter for measuring the effectiveness of each retrofit option. In this paper, the expected life cycle cost is estimated as (Wen 2001):

$$\mathbb{E}[C] = C_0 + C_{\mathrm{R}} + C_{\mathrm{M}} \tag{11}$$

where C_0 is the initial construction or upgrade installation cost (Miano et al. 2017 a), C_{R} is the repair cost considering also the downtime loss, and C_{M} is the annual maintenance costs. The repair cost C_{R} is equal to:

$$C_{\mathrm{R}} = \sum_{t=0}^{T} \sum_{pl=1}^{N_{PL}} PLC \cdot e^{-\lambda_{\mathrm{d}} t} \left[P\left(PL \,|\, [t, t+1]\right) - P\left(PL+1 \,|\, [t, t+1]\right) \right] \tag{12}$$

where N_{PL} is the number of prescribed performance levels; *PLC* is the expected cost of restoring the structure from the *pl*th performance level back to its intact state; λ_{d} is the annual discount rate and $\exp(-\lambda_{\mathrm{d}} t)$ denotes the change in the monetary-based evaluations per time; $P(PL|[t,\ t+1])$ is the probability of exceeding the *pl* in time interval [t, t+1]. $P(PL[t,\ t+1])$ can be calculated as:

$$P\left(PL \,|\, [t, t+1]\right) = \lambda_{pl} \exp\left(-\lambda_{pl} t\right) \tag{13}$$

where λ_{pl} is the mean annual rate of exceeding the performance level *pl* and can be calculated from the following closed-form expression (Jalayer and Cornell 2003):

$$\lambda_{pl} = \lambda_{S_a}\left(\eta(S_a^{\,DCR_{PL}=1})\right) \cdot \exp\left((k^2/2) \cdot \beta(S_a^{\,DCR_{PL}=1})^2\right) \tag{14}$$

where $\lambda_{\mathrm{Sa}}(\eta(S_a^{DCRPL=1}))$ is the hazard value for the median Sa at the onset of *pl*. *PLC* is equal to:

$$PLC = DTC \cdot e^{-\lambda_{\mathrm{d}} \tau_{pl}} + RC_{pl} \tag{15}$$

where *DTC* is the annual cost of downtime; τ_{pl} is the repair time and RC_{pl} is the replacement cost associated with desired *pl*th performance level. The cost of maintenance C_M can be estimated as:

$$C_{\mathrm{M}} = \int_0^{t_{life}} C_{\mathrm{m}} e^{-\lambda_{\mathrm{d}} t} dt = (C_{\mathrm{m}} / \lambda_{\mathrm{d}}) \cdot [1 - e^{-\lambda_{\mathrm{d}} t_{life}}] \tag{16}$$

where C_m is the constant annual maintenance cost. In Miano et al. 2017 a, the values adopted for C_o (Liel et al. 2013, and Vitiello et al. 2016, Comerio 2006), *DTC* (Jalayer et al. 2012), RC_{IO}, RC_{LS}, RC_{CP} (Liel et al. 2013, FEMA 2003) and C_m (Ebrahimian et al. 2015) are

presented in details. Figure 9 shows the expected life-cycle cost for bare frame and for the alternative retrofit schemes included in the comparison, i.e., the retrofit schemes for which the demand is lower than the capacity for all the performance levels (Table 1).

It can be observed that FRP wrapping (b) is the most convenient option economically-speaking after 20 years, while RC jacketing (a) becomes the most convenient option after 50 years. Making the assumption of a residual life greater than 50 years, RC jacketing (a) seems to be the most suitable strategy based on life cycle cost considerations, while if the residual life is fixed to be smaller than 50 years, FRP wrapping (b) becomes the best retrofit scheme.

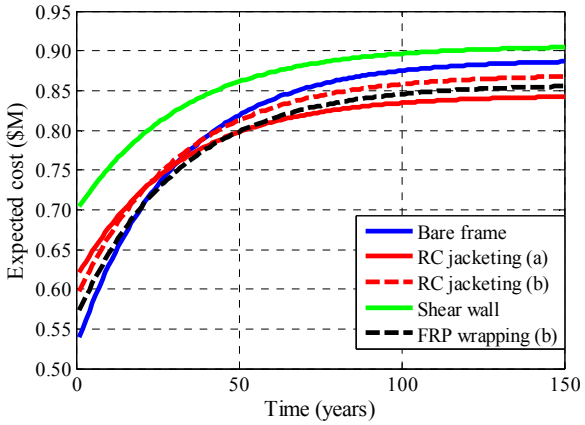

Figure 9. The expected life-cycle cost for bare frame and alternative retrofit schemes.

5. CONCLUSIONS

In this paper, alternative retrofit methods are compared for the case study frame, modeled considering the effect of flexural-shear-axial load interaction to capture column shear and axial failures. As nonlinear dynamic analysis, Cloud Analysis considering the cases of collapse and/or global dynamic instability is used which exclusively employs un-scaled ground motion time histories. A framework for probability-based demand and capacity factor design (*DCFD*) seismic safety evaluation is implemented in order to verify the structural performance and safety at each chosen performance level. In summary, the proposed methodology can be used to select the optimal retrofit strategy by comparing the loss expected during the service life based on risk-related safety-checking criteria. In particular, the methodology identifies the most economic retrofit solution that satisfies structural safety requirements for a given performance level. The only compatibility requirement among alternative retrofit solutions is a uniform definition of the onset of performance level(s). Retrofit design criteria such as target drift capacity (adopted in this work) and target strength are very helpful in terms of feeding an intelligent "first guess" into the procedure. Such a first guess is going to be assessed based on performance-based criteria. In other words, the performance-based retrofit assessment procedure rules out the proposed strategies that do not meet the code-based (or desirable) structural safety criteria. In conclusion, the whole performance-based procedure can be formalized as an optimization procedure that minimizes/maximizes a utility function (e.g., economic losses, functional benefits, etc.) and satisfies code-based (or desirable) safety constraints.

ACKNOWLEDGMENTS

The first author visited the Ohio State University to conduct part of the presented research. His visit was funded by the University of Naples Federico II. This support is gratefully acknowledged.

REFERENCES

ASCE (American Society of Civil Engineers). (2013). *Seismic Evaluation and Retrofit of Existing Buildings, ASCE/SEI 41-13*, Reston, VA, 2014.

Baker, J. W., and Cornell, C. A. (2005). "A vector□valued ground motion intensity measure consisting of spectral acceleration and epsilon." Earthq Eng & Struct Dyn **34(10)**, 1193-1217.

Celik, O.C. and Ellingwood, B.R. (2010). "Seismic fragilities for non-ductile reinforced concrete frames–Role of aleatoric and epistemic uncertainties." Struct Safety 32(1), 1-12.

Comerio, M.C. (2006). "Estimating downtime in loss modeling." Earthq Spectra, 22.2, 349-365.

Cornell, C.A. and Krawinkler H. (2000). "Progress and challenges in seismic performance assessment." PEER Center News, 3(2), 1-2.

Cornell, C. A., Jalayer, F., Hamburger, R. O., and Foutch, D. A. (2002). "Probabilistic basis for 2000 SAC federal emergency management agency steel moment frame guidelines." J Struct Eng, 128(4), 526-533.

Eads, L., Miranda, E., Krawinkler, H., and Lignos, D. G. (2013). "An efficient method for estimating the collapse risk of structures in seismic regions." Earthq Eng & Struct Dyn, 42(1), 25-41.

Ebrahimian, H., Jalayer, F., and Manfredi G. (2015). "Seismic retrofit decision-making of bridges based on life-cycle cost criteria*." Proc., 5th ECCOMAS Thematic Conference on Computational Methods in Struct Dyn & Earthq Eng*, Crete, Greece, 25-27 May 2015.

Elwood, K.J., Moehle, J.P. (2005). "Axial capacity model for shear-damaged columns." ACI Struct J, 102, 578-587.

Fardis, M.N. (2009). "Seismic design, assessment and retrofitting of concrete buildings based on EN-Eurocode 8." Vol. 8, Springer Science & Business Media.

FEMA, HAZUS-MH., (2003). MR3 Technical Manual. *Multi-hazard Loss Estimation Methodology Earthquake Model*, Washington (DC), 2003.

Gerin, M., and Adebar, P. (2004). "Accounting for shear in seismic analysis of concrete structures." Proc, 13th World Conference on Earthq Eng, Vancouver, Canada, 1-6 August, 2004.

Galanis, P.H., and Moehle, J.P. (2015). "Development of Collapse Indicators for Risk Assessment of Older-Type Reinforced Concrete Buildings." Earthq Spectra, 31(4), 1991-2006.

Jalayer F., and Cornell C. A. (2003). "A technical framework for probability-based demand and capacity factor design (DCFD) seismic formats." Technical Report PEER 2003/08, Berkeley, USA.

Jalayer, F., Franchin, P., and Pinto, P. (2007). "A scalar damage measure for seismic reliability analysis of RC frames." Earthq Eng & Struct Dyn, 36(13), 2059-2079.

Jalayer, F. and Cornell, C.A. (2009). "Alternative non□linear demand estimation methods for probability□based seismic assessments." Earthq Eng & Struct Dyn, 38(8), 951-972.

Jalayer, F., Asprone, D., Chiodi, R., Prota, A., and Manfredi, G. (2012). "Seismic Retrofit Decision-Making based On Life Cycle Cost Criteria." Proc, 15th word conference on Earthq Eng, Lisbon, Portugal, 24-28 September 2012.

Jalayer F, De Risi R, and Manfredi G. (2015). "Bayesian Cloud Analysis: efficient structural fragility assessment using linear regression." Bull Earthq Eng, 13(4), 1183-1203.

Jalayer, F., Carozza, S., De Risi, R., Manfredi, G., and Mbuya, E. (2016). "Performance-based flood safety-checking for non-engineered masonry structures." Eng Struct, 106, 109-123.

Jalayer, F., and Ebrahimian H. (2017). “Seismic risk assessment considering cumulative damage due to aftershocks.” Earthq Eng & Struct Dyn, 46(3), 369-389.
Jalayer, F., Ebrahimian, H., Miano, A., Manfredi, G., and Sezen H. (2017). “Analytical fragility assessment using un-scaled ground motion records.” Earthq Eng & Struct Dyn, https://doi.org/10.1002/eqe.2922.
Krawinkler, H. (2005). “Van Nuys hotel building testbed report: exercising seismic performance assessment.” *Technical Report PEER 2005/11*, Berkeley, USA.
Liel, A. B., Haselton, C.B., Deierlein, G.G., and Baker, J.W. (2009). “Incorporating modeling uncertainties in the assessment of seismic collapse risk of buildings.” Struct Safety, 31(2), 197-211.
Liel, A.B., and Deierlein G.G. (2013). “Cost-benefit evaluation of seismic risk mitigation alternatives for older concrete frame buildings.” Earthq Spectra, 29(4), 1391-1411.
McKenna, F. (2011). “OpenSees: a framework for earthquake engineering simulation.” Comp in Sc & Eng, 13(4), 58-66.
Miano, A., Sezen, H., Jalayer, F., and Prota, A., (2017)a. “Performance based assessment methodology for retrofit of buildings.” Earthq Spectra, (Under Review).
Miano, A., Sezen, H., Jalayer, F., and Prota, A. (2017)b. “Performance based comparison of different retrofit methods for reinforced concrete structures.” Proc of the 6th ECCOMAS Thematic Conference on Computational Methods in Struct Dyn & Earthq Eng, Rhodes, Greece, 15-17 June 2017.
Moehle, J.P. (2000). “State of research on seismic retrofit of concrete building structures in the US.” In US-Japan symposium and workshop on seismic retrofit of concrete structures.
Scott M.H., and Fenves G.L. (2006). “Plastic hinge integration methods for force-based beam–column elements.” J Struct Eng, 132(2), 244-252.
Setzler, E.J., and Sezen, H. (2008). “Model for the lateral behavior of reinforced concrete columns including shear deformations.” Earthq Spectra, 24(2), 493-511.
Sezen, H., Whittaker, A., Elwood, K., and Mosalam, K. (2003). “Performance of reinforced concrete buildings during the August 17, 1999 Kocaeli, Turkey earthquake, and seismic design and construction practise in Turkey.” Eng Struct, 25(1), 103-114.
Sezen, H., and Moehle, J.P. (2003). “Bond-slip behavior of reinforced concrete members.” Fib Symposium on Concrete Structures in Seismic Regions, CEB-FIP, Athens, Greece.
Sezen, H., and Moehle, J.P. (2004). “Shear strength model for lightly reinforced concrete columns.” J Struct Eng, 130(11), 1692-1703.
Sezen, H. (2008). “Shear deformation model for reinforced concrete columns.” Struct Eng and Mechanics, 28(1), 39-52.
Shome N., Cornell C.A., Bazzurro P., and Carballo J.E. (1998). "Earthquakes, records, and nonlinear responses." Earthq Spectra, 14(3), 469-500.
Thermou, G.E., and Elnashai, A.S. (2006). "Seismic retrofit schemes for RC structures and local□global consequences." Progress in Struct Eng and Materials, 8.1: 1-15.
Trifunac, M.D., Ivanovic, S.S., and Todorovska, M.I. (1999). "Instrumented 7-storey reinforced concrete building in Van Nuys, California: description of the damage from the 1994 Northridge Earthquake and strong motion data." Report CE 99 2.
Vamvatsikos, D., and Cornell, C.A. (2002). "Incremental dynamic analysis." Earthq Eng & Struct Dyn, 31(3), 491-514.
Vitiello, U., Asprone, D., Di Ludovico, M., and Prota, A. (2017). "Life cycle cost optimization of the seismic retrofit of existing RC structures." Bull Earthq Eng, 15.5, 2245-2271.
Wen, Y.K. (2001). “Reliability and performance-based design.” Struct Safety, 23(4), 407-428.
Zareian, F., and Krawinkler, H. (2007). “Assessment of probability of collapse and design for collapse safety.” Earthq Eng & Struct Dyn, 36(13), 1901-1914.